Response to Referee #4

This work by Zhang et al. (2026) assesses the impacts of incorporating additional isoprene chemistry into CAM6-Chem. Isoprene's low-NOx pathway was updated and a high-NOx pathway was introduced. Comparison with observational data revealed improvements in composition and isoprene-derived secondary organic aerosol (ISOA) representation. A spatial analysis, which revealed opposite trends in different regions, provided insight into the weak national-mean ISOA trend in China. This study addressed a relevant and important research question and conducted a broad range of analyses to substantiate the claim that their updates to the CAM6-Chem isoprene oxidation mechanism led to improved ISOA representation over China. Clarity could be improved in some areas and some figures require editing.

We are very grateful to the reviewer for the constructive evaluation and helpful suggestions, which have allowed us to clarify and improve the manuscript. Before addressing the reviewer's comments point by point, we briefly summarize the major revisions made in response to Referee #4. The reviewer's comments are shown in **bold blue text**, while our responses and the corresponding revised manuscript text are shown in black text. Line numbers refer to the revised manuscript.

In response to Referee #4, we revised the treatment and discussion of AIEOSN and other OSN-like products by replacing the initially submitted parallel-sink implementation with the updated relative-rate branching framework, which substantially reduces the simulated inorganic-nucleophile-addition product contributions and improves consistency with molecular tracer observations. We also clarified the calculation of OA/SOA normalized mean biases using site- and period-matched model–observation pairs, and revised the interpretation of the bulk OA/SOA improvement to emphasize that other SOA pathways were not modified. In addition, we expanded the definitions of model species and reaction pathways, clarified the meaning of key terms and figure elements, and revised several figures and tables to improve readability.

Major Comments

Comment#1: This study assesses the impact of expanding the representation of ISOA subspecies in CAM6-Chem from one to four. Though it is briefly mentioned that "discrepancies in the fractional contributions of individual species" exist between the observed and modeled ISOA subspecies, more thoroughly addressing the significant overestimation in AIEOSN is necessary. Why might this be occurring? Since AIEOSN is the only ISOA subspecies present in the pre-updated and updated model, it might be insightful to show a comparison of AIEOSN concentrations before and after the update, if possible.

Response: We thank the reviewer for raising this important point. We agree that the previously simulated AIEOSN contribution required further clarification. As also discussed in our response to the second sub-question of Reviewer #3, Comment #2, the apparent overestimation of AIEOSN was mainly associated with how the updated epoxide-derived ISOA mechanism was implemented in the original submission. In the initially submitted implementation, ISOA formation pathways for IEPOX, HMML, and MAE were represented as multiple parallel heterogeneous uptake reactions. Each product-forming pathway directly consumed the same gas-phase epoxide precursor using a distinct channel-specific reactive

uptake coefficient derived from its respective aqueous-phase rate expression. As a result, ISOA speciation was effectively determined at the level of independent uptake fluxes, rather than being constrained by a single total uptake rate followed by internal partitioning among competing reaction channels. This approach allowed each channel to act as an independent sink of the precursor and resulted in the inorganic-nucleophile addition channel receiving an artificially enhanced share of gas-phase precursor uptake flux, leading to an overestimation of the corresponding inorganic-nucleophile addition products such as AIEOSN and AHMOSN.

To address this issue, we revisited the treatment of epoxide-derived product formation and revised the model implementation using a relative-rate branching framework following Budisulistiorini et al. (2017). In essence, the implementation used in the original submission treated epoxide uptake as multiple parallel sinks, whereas the revised implementation treats epoxide uptake as a single total uptake process followed by competitive branching into different product classes.

In the revised implementation, a single total pseudo-first-order aqueous-phase rate constant $k_{aq,total}$ is first calculated as the sum of the particle-phase reaction channels (H_2O-mediated nucleophilic addition and inorganic-nucleophile addition channels) considered here: $k_{aq,total} = k_{H^+}[H^+] + k_{nuc}([SO_4^{2-}] + [NO_3^-])[H^+] + k_{HSO_4^-}[HSO_4^-]$. This total rate is used to compute the reactive uptake coefficient (γ) and the total uptake flux for each precursor. ISOA speciation is then determined diagnostically by partitioning the total uptake flux according to the fractional contribution of each reaction channel to $k_{aq,total}$. Specifically, the branching ratio for the H_2O-mediated nucleophilic addition product class is calculated as $k_{aq,H_2O}/k_{aq,total} = k_{H^+}[H^+]/(k_{H^+}[H^+] + k_{nuc}([SO_4^{2-}] + [NO_3^-])[H^+] + k_{HSO_4^-}[HSO_4^-])$, whereas the branching ratio for the inorganic-nucleophile-addition product class is calculated as $k_{aq,SO_4/NO_3/HSO_4}/k_{aq,total} = (k_{nuc}([SO_4^{2-}] + [NO_3^-])[H^+] + k_{HSO_4^-}[HSO_4^-])/(k_{H^+}[H^+] + k_{nuc}([SO_4^{2-}] + [NO_3^-])[H^+] + k_{HSO_4^-}[HSO_4^-])$. The total particle-phase ISOA production is then distributed into H_2O-mediated nucleophilic addition products and inorganic-nucleophile addition products according to these branching ratios. This treatment ensures that the total uptake of each precursor is governed by the full particle-phase reaction rate constant, while the product distribution reflects the relative competition among nucleophilic addition pathways. This treatment is analogous to Budisulistiorini et al. (2017), who determined IEPOX-SOA speciation between tetrols and organosulfates based on the relative rates of precursor conversion to these products.

This revision substantially changes the simulated product distribution. As shown in Figure R1, the initially submitted implementation produced a relatively large contribution from AIEOSN and AHMOSN, whereas the revised relative-rate branching treatment greatly reduces their simulated contributions. In the revised implementation, AIETET becomes the dominant simulated ISOA product at Beijing, Hefei, and Kunming, and the combined contribution of AIEOSN and AHMOSN is reduced to only a few percent. This revised product distribution is more consistent with the molecular tracer observations used for model evaluation and with previous field measurements showing relatively small AIEOSN

contributions, such as He et al. (2018). Broader changes in total concentrations, interannual variability, long-term trends, and attribution coefficients resulting from this implementation update are described in the response to the second sub-question of Reviewer #3, Comment#2.

We have also revised the relevant description in the manuscript to clarify that the earlier CAM6-Chem configuration described by Zhang et al. (2025) represented the low-NOx IEPOX pathway as a lumped ($ISOA_{IEPOX}$) product, whereas the explicit ISOA representation adopted in this study resolves epoxide-derived ISOA into product classes associated with H_2O-mediated and inorganic-nucleophile addition pathways and also includes high-NOx epoxide precursors. We appreciate the reviewer's suggestion to compare AIEOSN before and after the update. In response, Figure R1 presents the initially submitted-versus-revised product distribution, which directly shows the reduction in the AIEOSN contribution together with the corresponding redistribution among other ISOA product classes. We believe this composition-based comparison provides a clearer way to illustrate the effect of the revised product-allocation treatment, because the main change occurs in the partitioning of epoxide-derived ISOA among product classes.

We have revised the corresponding model-observation comparison in the manuscript and present the comparison between the initially submitted and revised results in Figure R1 of this response. We also added discussion in Sect. 3.1 and Sect. 4 to clarify the remaining uncertainties associated with the representation of epoxide-derived product formation. Although the revised branching treatment substantially reduces the AIEOSN and AHMOSN contributions simulated in the initially submitted implementation, remaining discrepancies between simulated and observed individual product fractions may still reflect uncertainties in pathway branching, reactive uptake parameters, mass transfer, aerosol phase state, and possible missing competing formation or loss processes. In particular, assumptions related to the core-shell uptake treatment, organic-shell viscosity, phase separation, product volatility, and the limited compound-specific constraints for HMML/MAE may affect the simulated abundance and partitioning of individual ISOA products. Future improvements will require better observational and laboratory constraints on epoxide-specific uptake parameters, aerosol phase state and diffusion limitations, product yields and volatility, as well as improved representation of potential non-epoxide ISOA formation pathways under atmospherically relevant aerosol conditions. These revisions have been incorporated in Sect. 3.1 (lines 299−314) and Sect. 4 (lines 659−677).

Budisulistiorini, S. H., Nenes, A., Carlton, A. G., Surratt, J. D., McNeill, V. F., and Pye, H. O. T.: Simulating aqueous-phase isoprene-epoxydiol (IEPOX) secondary organic aerosol production during the 2013 Southern Oxidant and Aerosol Study (SOAS), Environ. Sci. Technol., 51, 5026–5034, https://doi.org/10.1021/acs.est.6b05750, 2017.

He, Q.-F., Ding, X., Fu, X.-X., Zhang, Y.-Q., Wang, J.-Q., Liu, Y.-X., Tang, M.-J., Wang, X.-M., and Rudich, Y.: Secondary organic aerosol formation from isoprene epoxides in the Pearl River Delta, South China: IEPOX- and HMML-derived tracers, J. Geophys. Res.-Atmos., 123, 6999–7012, https://doi.org/10.1029/2017JD028242, 2018.

Zhang, W., Liu, Y., Yue, M., Dong, X., Huang, K., and Wang, M.: Understanding the long-term trend of organic aerosol and the influences from anthropogenic emission and regional climate change in China, Atmos. Chem. Phys., 25, 3857–3872, https://doi.org/10.5194/acp-25-3857-2025, 2025.

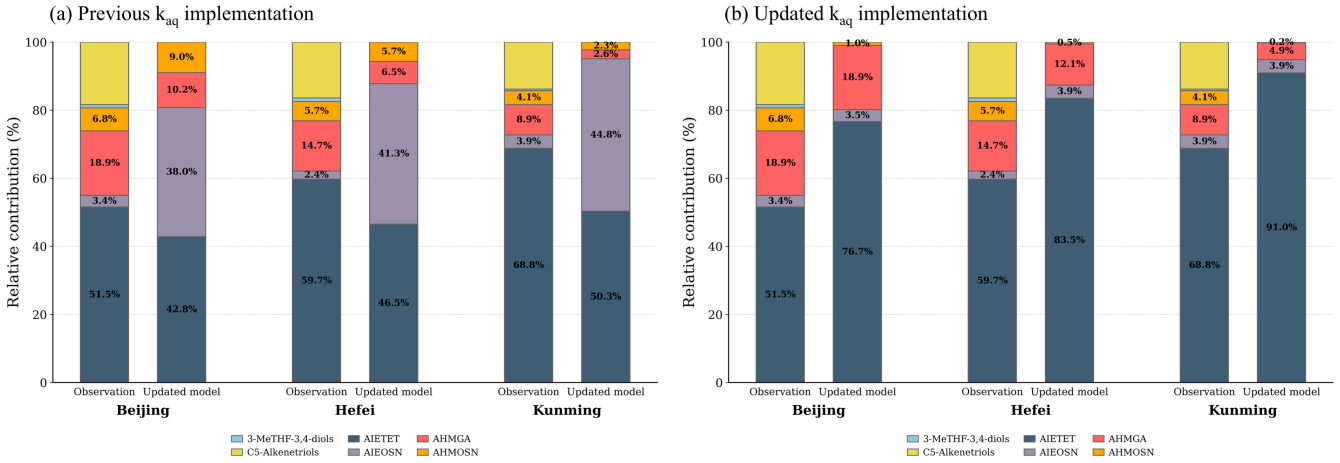

105

Figure R1: Comparison of ISOA product composition between ground-based observations adapted from Zhang et al. (2022) and the model simulation in this study, corresponding to the observation-model comparison shown in the original Figure 2c in the manuscript. The grouped stacked bars show the relative contribution of each ISOA product to total measured or simulated ISOA at Beijing, Hefei, and Kunming. For each city, the left bar represents the observed composition and the right bar represents the 110 **corresponding model simulation. Panel (a) shows results obtained with the previous k_{aq} implementation, in which product-forming pathways were treated as independent uptake sinks. Panel (b) shows results obtained with the updated k_{aq} implementation, in which total epoxide uptake is first calculated and then partitioned among product classes using the relative-rate branching framework.**

Lines 299−314:

115 Several factors may contribute to these positive biases. First, missing or simplified competing loss pathways may cause an over-allocation of epoxide precursors to the explicitly represented ISOA products. For example, a fraction of IEPOX-derived products in the real atmosphere may be diverted to C5-alkene triols or other particle-phase products that are not explicitly represented here, thereby reducing the effective yield of AIETET (Pye et al., 2013). In addition, previous studies have shown that AIETET and AHMGA are sensitive to factors such as pathway branching, mass transfer, reaction kinetics, and aerosol 120 phase state. For example, uncertainties in the relative rates of water addition versus organosulfate formation can affect the predicted product distribution between 2-MT and organosulfate products (Budisulistiorini et al., 2017). Similarly, assumptions related to aerosol phase state, organic-shell viscosity, and phase separation can influence IEPOX reactive uptake and may affect the simulated abundance of IEPOX-derived tracers (Zhang et al., 2018, 2019; Chen et al., 2024b). In particular, the current core-shell uptake treatment assumes the same reaction rate coefficient in the organic shell and aqueous 125 core. If phase separation and viscous organic coatings impose stronger diffusion limitations than represented here, effective epoxide uptake may be reduced in the real atmosphere, and the model may overestimate ISOA formation, especially under conditions with high organic coatings or strong phase separation. For AHMGA, uncertainties in the multiphase uptake and reaction parameters of HMML/MAE may also contribute to the model bias, because compound-specific constraints for these high-NOx epoxides remain limited (Zhang et al., 2022; Zhu et al., 2025).

130 **Lines 659−677:**

Future model development should further address several simplifying assumptions in the current epoxide reactive uptake parameterization. As described in Sect. 2.1.2, the model follows a core-shell treatment in which the organic shell and aqueous core are assumed to have the same reaction rate coefficient. Because phase separation and increased organic-shell viscosity can limit epoxide diffusion and reactive uptake, this assumption may overestimate epoxide-derived ISOA under strongly phase-separated or highly viscous conditions (Zhang et al., 2019; Schmedding et al., 2020; Chen et al., 2024b; Farrell et al., 2025). HMML and MAE are also represented using the same solubility, diffusivity, and condensed-phase reaction parameters as IEPOX because compound-specific laboratory constraints remain limited. This IEPOX-like treatment introduces uncertainty in the absolute uptake rates of high-NOx epoxides and in the quantitative $ISOA_{HMML+MAE}/ISOA_{IEPOX}$ ratio. The assumptions of 100% ISOA yield from epoxide reactive uptake and non-volatile epoxide-derived ISOA introduce additional uncertainty, although they are consistent with previous global ISOA modeling studies (Marais et al., 2016; Jo et al., 2019, 2021). Lower effective yields or partial volatility, especially for products such as 2-MT and 2-MGA, could reduce simulated ISOA concentrations and their sensitivity to sulfate, aerosol liquid water, and acidity. Consistent with this need, gas–particle partitioning treatments for 2-MT in regional models suggest a useful direction for future improvement in global models (Pye et al., 2018; Shrivastava et al., 2022). Finally, the removal of ISOA formation from the VBS scheme may also remove important non-epoxide contributions to ISOA that were previously represented implicitly, such as multifunctional organic peroxides under low-NOx conditions and organic nitrates under high-NOx conditions (Paulot et al., 2009a; Schwantes et al., 2019). Taken together, these assumptions mean that the long-term trends and regression-based attributions diagnosed here should be interpreted within the adopted epoxide-focused chemical framework, rather than as exact causal contributions independent of model structure and parameterization.

Comment#2: The conclusion that the model updates improved SOA and OA representation is strongly substantiated by the comparison of normalized mean biases (NMB) with and without the updated isoprene chemistry. These NMB are calculated with observational OA/POA/SOA data from across China during 2013-2019. It may be helpful to expand on the calculation of these NMB (in [Lines 251-252]), given the different time periods and site-specific measurements. In [Line 251], the improvement of SOA representation is said to be "mainly owing to improved ISOA simulation". This implies that there may be other factors contributing to this improvement. If this is the case, it would be helpful to expand on this further.

Response: We thank the reviewer for these helpful suggestions. We have expanded the description of the NMB calculation in Sect. 3.1 to improve clarity. We now provide a general explanation before presenting these statistics. Specifically, for the OA/SOA evaluation, model outputs were sampled at the corresponding observational site locations and averaged over the same observational periods before calculating the model-observation differences. The paired model and observational values from different sites and time periods were then combined across all paired samples to calculate the NMB, thereby accounting for the site-specific locations and different temporal coverage of the observational datasets.

We also revised the statement regarding the improvement in SOA representation. We agree that the previous wording "mainly owing to improved ISOA simulation" could imply that other SOA formation pathways were also modified. In the

revised manuscript, we clarify that the mechanism update implemented in this study focuses on ISOA formation, while other SOA formation pathways were not modified. Therefore, the improvement in bulk SOA representation is attributed to the enhanced representation of ISOA in the updated model. These revisions have been incorporated in Sect. 3.1 (lines 288−292 and lines 327−329).

Lines 288−292:

For all normalized mean biases (NMB) calculations in this section, model outputs were sampled at the corresponding observational site locations and averaged over the same observational periods before calculating the model-observation differences. The paired model and observational values from different sites and time periods were then combined across all paired samples to calculate the NMB, thereby accounting for the site-specific locations and different temporal coverage of the observational datasets.

Lines 327−329:

This improvement reflects the enhanced representation of ISOA formation introduced in this study, since other SOA formation pathways were not modified relative to the earlier CAM6-Chem configuration.

Technical Corrections/Suggestions

Comment#3: [Line 142] Need to define "MACR".

Response: We thank the reviewer for pointing this out. We have revised Sect. 2.1.2 to define MACR when it first appears. This revision has been incorporated in Sect. 2.1.2 (line 168−170).

Line 168−170:

Methacrolein (MACR), the precursor of MPAN in the high-NOx pathway, is formed following the default MOZART-TS2 mechanism. The reaction of MPAN with OH yields HMML and MAE, with molar branching ratios of 0.75 and 0.02, respectively, based on the experimental results reported by Nguyen et al. (2015) (Table S2).

Comment#4: [Eq 4] Need to define "k_org".

Response: We thank the reviewer for pointing this out. We have revised Sect. 2.1.2 to explicitly define k_{org} as the pseudo-first-order reaction rate constant of epoxides in the organic shell (s^{-1}). We further clarify that, following Jo et al. (2021), the reactivity of epoxides in the organic shell is parameterized using the same reaction rate constant as in the aqueous core, so $k_{org}=k_{aq,total}$. This revision has been incorporated in Sect. 2.1.2 (lines 212−214 and Lines 235−240).

Jo, D. S., Hodzic, A., Emmons, L. K., Tilmes, S., Schwantes, R. H., Mills, M. J., Campuzano-Jost, P., Hu, W., Zaveri, R. A., Easter, R. C., Singh, B., Lu, Z., Schulz, C., Schneider, J., Shilling, J. E., Wisthaler, A., and Jimenez, J. L.: Future changes in isoprene-epoxydiol-derived secondary organic aerosol (IEPOX SOA) under the Shared Socioeconomic

Pathways: the importance of physicochemical dependency, Atmos. Chem. Phys., 21, 3395–3425, https://doi.org/10.5194/acp-21-3395-2021, 2021.

Lines 212−214:

Where R_C is the inorganic aqueous core radius (m), k_{org} is the pseudo-first-order reaction rate constant of epoxides in the organic shell (s^{-1}), and $k_{aq,total}$ is the total pseudo-first-order aqueous-phase reaction rate constant (s^{-1}), calculated as the sum of all particle-phase reaction channels that consume each precursor

Lines 235−240:

This study follows the approach of Jo et al. (2021), where the reactivity of epoxides in the organic shell was parameterized with the same reaction rate constant as in the aqueous phase ($k_{org}=k_{aq,total}$). This treatment follows the Jo et al. (2019, 2021) core-shell framework and represents a simplifying assumption, because phase separation, organic-shell viscosity, and differences in acidity between the inorganic core and organic shell may alter epoxide diffusion and reactivity (Schmedding et al., 2020; Farrell et al., 2025).

Comment#5: [Lines 192-195] I'm assuming AIETET, AIEOSN, AHMGA, AHMOSN stand for Aerosol from IEPOX – tetrols, Aerosol from IEPOX – organosulfate/nitrate, Aerosol from HMML/MAE – glyceric acid, and Aerosol from HMML/MAE – organosulfate/nitrate. It'd be helpful to explicitly include this so readers can more easily understand the subsequent references/analyses. Could these be named something more intuitive? Such as AIEAQ, AIEOSN, AHMAQ, AHMOSN? Referring to IEPOX's and HMML/MAE's aqueous and organosulfate/nitrate pathways?

Response: We thank the reviewer for this helpful suggestion. We agree that the meanings and formation pathways of AIETET, AIEOSN, AHMGA, and AHMOSN should be stated more explicitly to help readers understand the subsequent analyses. In the revised manuscript, we have added a clearer definition of these four ISOA subspecies when they are first introduced.

Specifically, we now clarify that ISOA formed from the heterogeneous uptake of IEPOX is divided into two product classes: 2-methyltetrols (2-MT; AIETET), produced through the H_2O-mediated nucleophilic addition channel, and organosulfate/organonitrate products (AIEOSN), produced through the inorganic-nucleophile addition channel. Similarly, ISOA formed from HMML and MAE is divided into 2-methylglyceric acid (2-MG; AHMGA), produced through the H_2O-mediated nucleophilic addition channel, and organosulfate/organonitrate products (AHMOSN), produced through the inorganic-nucleophile addition channel.

We appreciate the reviewer's suggestion to consider more intuitive names. However, we have retained the original species names, AIETET, AIEOSN, AHMGA, and AHMOSN, because they correspond directly to the model species used in the implementation and encode both the precursor source and the product type. Specifically, "A" denotes aerosol-phase products, "IE" denotes IEPOX-derived products, "HM" denotes HMML/MAE-derived products, "TET" denotes 2-methyltetrols, "GA"

denotes 2-methylglyceric acid, and "OSN" denotes organosulfate/organonitrate products. Therefore, rather than renaming the species, we revised the text to explicitly link each species name to its precursor, product class, and formation channel. This clarification has been added in Sect. 2.1.2 (lines 244−255).

Lines 244−255:

As illustrated in Fig. 1, the uptake-derived ISOA product classes are mapped to four model species. ISOA formed from the heterogeneous uptake of IEPOX is divided into two product classes: 2-MT (AIETET), produced through the H_2O-mediated nucleophilic addition channel, and organosulfate/organonitrate products (AIEOSN), produced through the inorganic-nucleophile addition channel. Similarly, ISOA formed from HMML and MAE is divided into 2-MG (AHMGA), produced through the H_2O-mediated nucleophilic addition channel, and organosulfate/organonitrate products (AHMOSN), produced through the inorganic-nucleophile addition channel. The ISOA yield from the reactive uptake of IEPOX, HMML, and MAE is assumed to be 100%, and ISOA derived from these epoxides is treated as non-volatile in the model. This assumption is in agreement with previous modeling studies (Budisulistiorini et al., 2017; Marais et al., 2016; Schmedding et al., 2019; Stadtler et al., 2018), which are based on field observations indicating that ISOA from these epoxides in the atmosphere exhibits very low volatility (Hu et al., 2016; Riva et al., 2019). Once ISOA from IEPOX, HMML, and MAE is formed, no further oxidation occurs in the model, consistent with previous studies (Budisulistiorini et al., 2017; Marais et al., 2016; Schmedding et al., 2019).

Comment#6: [Fig. 1] What is the difference between the dashed & solid arrows? Defining abbreviations in the figure caption would be helpful (at least for AeroWater, AIETET, AIEOSN, AHMGA, AHMOSN).

Response: We thank the reviewer for this helpful suggestion. We have revised the caption of Fig. 1 to clarify the meaning of the arrow styles and to define the abbreviations used in the schematic. The revised caption now states that dashed arrows indicate gas-phase reactions, whereas solid arrows indicate particle-phase heterogeneous uptake and product-formation reactions. We have also added definitions for the key abbreviations in the caption. Specifically, AeroWater denotes aerosol liquid water; AIETET denotes IEPOX-derived 2-methyltetrols; AIEOSN denotes IEPOX-derived organosulfate/organonitrate products; AHMGA denotes HMML/MAE-derived 2-methylglyceric acid; and AHMOSN denotes HMML/MAE-derived organosulfate/organonitrate products. In addition, we revised the caption wording to describe the color coding more clearly. Species explicitly represented as updated ISOA precursors or product classes in this mechanism are shown in green, and the explicitly represented ISOA formation pathways are shown in orange.

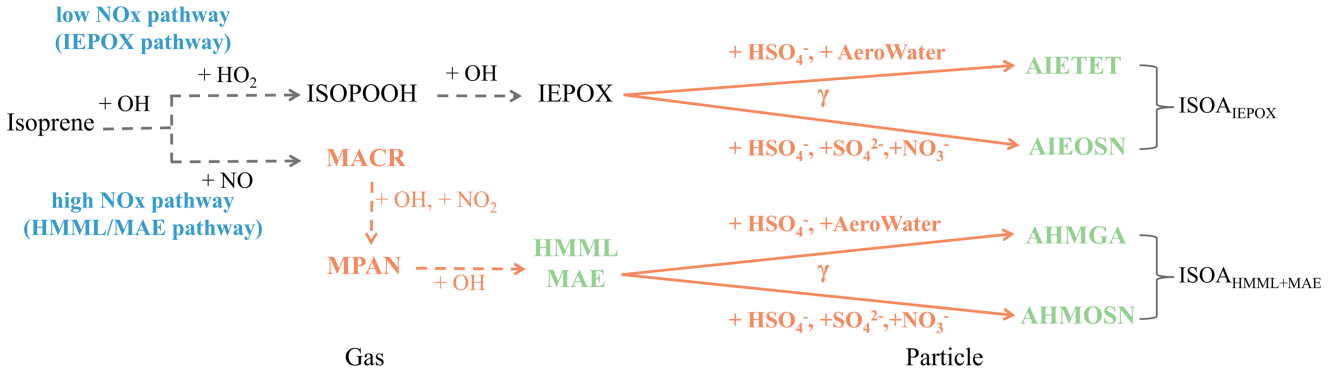

Figure 1: Schematic of the explicit isoprene-derived secondary organic aerosol (ISOA) formation mechanism implemented in CAM6-Chem in this study. Dashed arrows indicate gas-phase reactions, whereas solid arrows indicate particle-phase heterogeneous uptake and product-formation reactions. Species explicitly represented as updated ISOA precursors or product classes in this mechanism are shown in green, and the explicitly represented ISOA formation pathways are shown in orange. AeroWater denotes aerosol liquid water. AIETET denotes IEPOX-derived 2-methyltetrols, AIEOSN denotes IEPOX-derived organosulfate/organonitrate products, AHMGA denotes HMML/MAE-derived 2-methylglyceric acid, and AHMOSN denotes HMML/MAE-derived organosulfate/organonitrate products.

Comment#7: [Fig. 2a] It may be helpful to include a description of what the dark and light gray lines represent. I'd also modify this plot so that points aren't being cut off (as seen on the x-axis). As for the legend, it would be helpful to modify it so that data points aren't obscuring the text and so that the example markers in the legend can't be mistaken for actual data.

Response: Thank you for the detailed suggestions. We have revised Fig. 2(a) accordingly. First, we adjusted the axis limits to ensure that all markers are fully visible and are no longer cut off near the plot boundaries. Second, we moved the legend outside the plotting area to avoid obscuring the data points and to prevent the legend markers from being confused with actual observations. Third, we added a description of the reference lines in the figure caption: the dark gray solid line denotes the 1:1 line, and the light gray solid lines denote the factor-of-10 range.

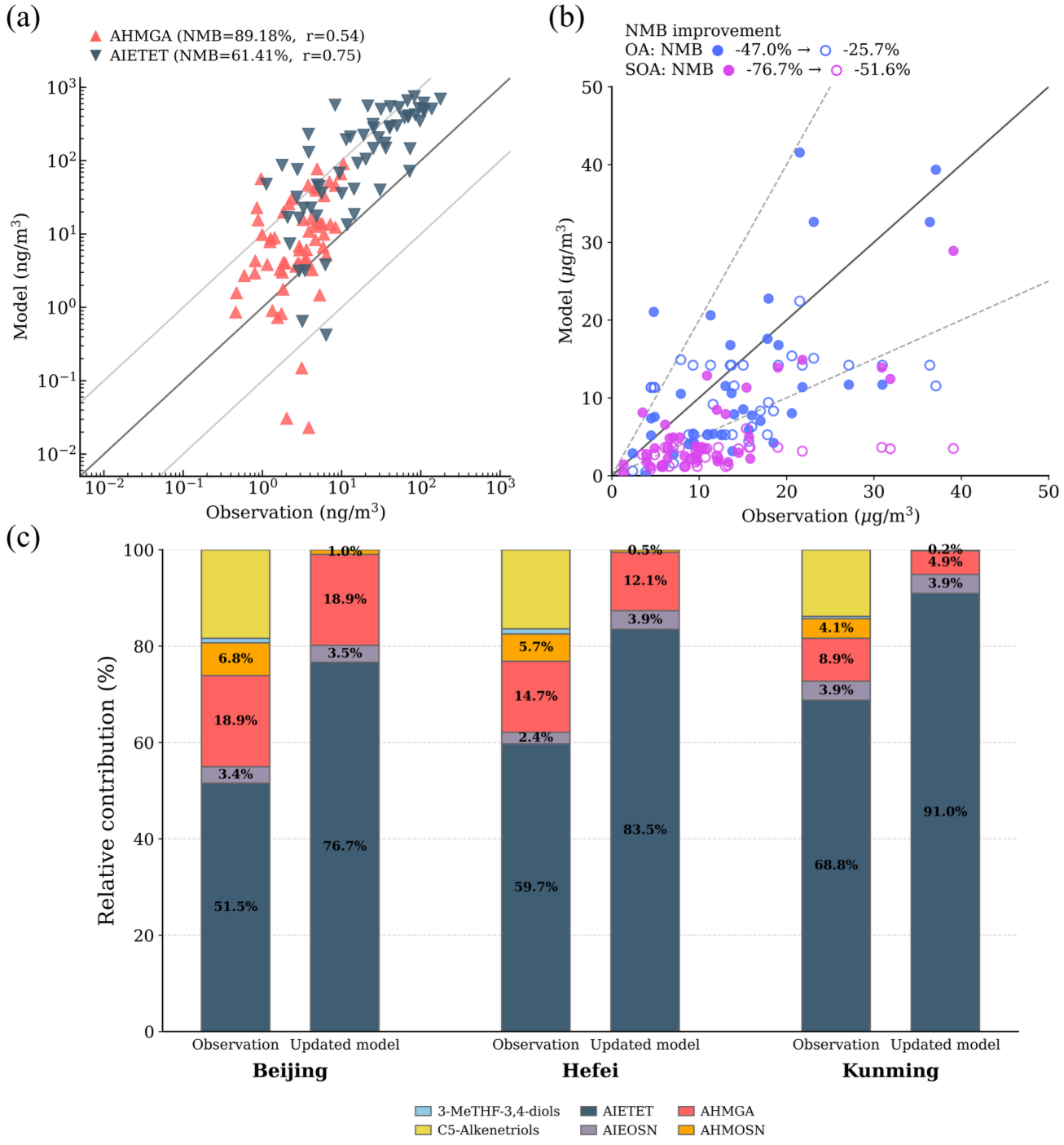

Figure 2: (a) Evaluation of simulated 2-methyltetrols (AIETET) and 2-methylglyceric acid (AHMGA) concentrations against ground-based observations from Ding et al. (2016) (ng m^{-3}). Statistical metrics were calculated using monthly means in log space. The dark gray solid line denotes the 1:1 line, and the light gray solid lines denote the factor-of-10 range. (b) Evaluation of simulated organic aerosol (OA) and secondary organic aerosol (SOA) concentrations before and after the mechanism update

against ground-based observations compiled from Miao et al. (2021) and Chen et al. (2024a) (μg m^{-3}). Filled circles represent simulations before the update, while open circles represent simulations after the update. Blue and magenta markers denote OA and SOA, respectively. The inset annotation summarizes the changes in normalized mean bias (NMB) from the original to the updated simulation. The dark gray solid line denotes the 1:1 line, and the light gray dashed lines denote the factor-of-two range. (c) Comparison of ISOA product composition between ground-based observations adapted from Zhang et al. (2022) and the updated model simulation in this study. The grouped stacked bars show the relative contribution of each ISOA product to total measured or simulated ISOA at Beijing, Hefei, and Kunming. For each city, the left bar represents the observed composition and the right bar represents the updated model.

Comment#8: [Fig. 2b] Same recommendation for legend as above. Include what the dark gray and light gray dashed lines represent in the figure caption.

Response: Thank you for the detailed suggestions. We have revised Fig. 2(b) following the same approach. The legend/annotation was reformatted and moved away from the main data region to avoid overlap with the plotted points. We also clarified the meaning of the reference lines in the figure caption. The dark gray solid line denotes the 1:1 line, and the light gray dashed lines denote the factor-of-two range.

Comment#9: [Fig. 2c] You specify what the rows represent in the figure caption; to be consistent, maybe do the same with the columns.

Response: Thank you for the suggestion. We have revised Fig. 2(c) and its caption to make the layout clearer. In the revised grouped stacked bar chart, each city forms one group, with the left bar showing the observed composition and the right bar showing the updated-model composition, as now explicitly stated in the caption.

Comment#10: [Fig. 3] Adding titles above each plot and enlarging colorbar titles would be helpful. For part c, I'd move the legend to the top so that "AHMGA" isn't obscured. Can you make a second legend circle size (in addition to the 60 ng/m^3 circle) that more closely resembles the largest pie chart in the plot?

Response: Thank you for the detailed suggestions. We have revised Fig. 3 accordingly. First, we added descriptive titles above each panel to clarify the information shown in Fig. 3. Second, we enlarged and clarified the colorbar labels in Fig. 3(a) and Fig. 3(b). For Fig. 3(c), we moved the species legend to the top of the panel so that all legend entries, including AHMGA, are clearly visible and no longer overlap with the map or pie charts. We also revised the pie-size reference. Instead of the original small 60 ng m^{-3} reference circle, we now use a larger 900 ng m^{-3} reference circle that better represents the size of the largest pie charts in the panel and improves interpretability. In addition, we lightened the map background and provincial boundaries to make the pie charts and regional labels more prominent.

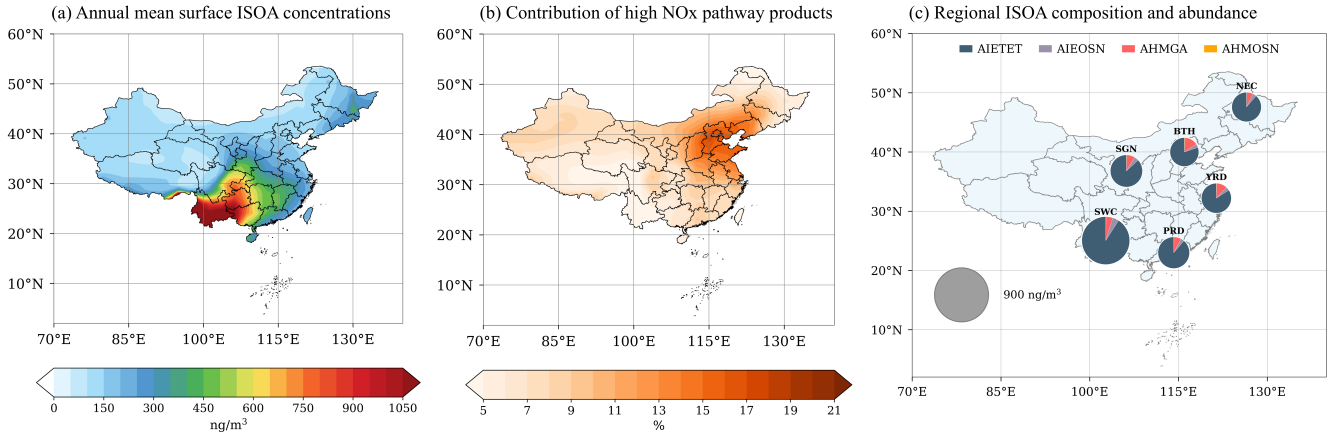

Figure 3: (a) Annual mean surface concentrations of isoprene-derived secondary organic aerosol (ISOA) over China, averaged over the five simulation years (2000, 2006, 2012, 2016, and 2019) (unit: ng m^{-3}). (b) Spatial distribution of the contribution of high-NOx pathway products, including 2-methylglyceric acid (AHMGA) and organosulfate/organonitrate products from the high-NOx pathway (AHMOSN), to annual mean total ISOA over China, averaged over the five simulation years (unit: %). (c) Composition of surface ISOA subspecies in six regions of China, including Southwest China (SWC), the Beijing–Tianjin–Hebei region (BTH), the Yangtze River Delta (YRD), the Pearl River Delta (PRD), the Shaanxi–Gansu–Ningxia region (SGN), and Northeast China (NEC), based on annual mean concentrations averaged over the five simulation years. Pie charts show the fractional contributions of individual ISOA subspecies, and the circle size represents the corresponding surface ISOA concentration (unit: ng m^{-3}).

Comment#11: [Fig. 4b] [OH] curve is missing! I'd clarify that you're referring to background aerosol properties (not ISOA properties) in the caption.

Response: We thank the reviewer for pointing this out. The OH curve was unintentionally omitted from Fig. 4(b) in the previous version. We have now added the standardized monthly variation of surface hydroxyl radical (OH) concentration to Fig. 4(b) and updated the legend accordingly.

We have also revised the caption of Fig. 4 to clarify that the variables shown in panel (b) represent background chemical and aerosol variables relevant to ISOA formation, rather than properties of ISOA itself. Specifically, the revised caption now refers to "background chemical and aerosol variables relevant to ISOA formation," including surface aerosol pH, surface sulfate concentration, surface aerosol liquid water mass concentration, and surface OH concentration. This revision has been incorporated in Fig. 4 and its caption.

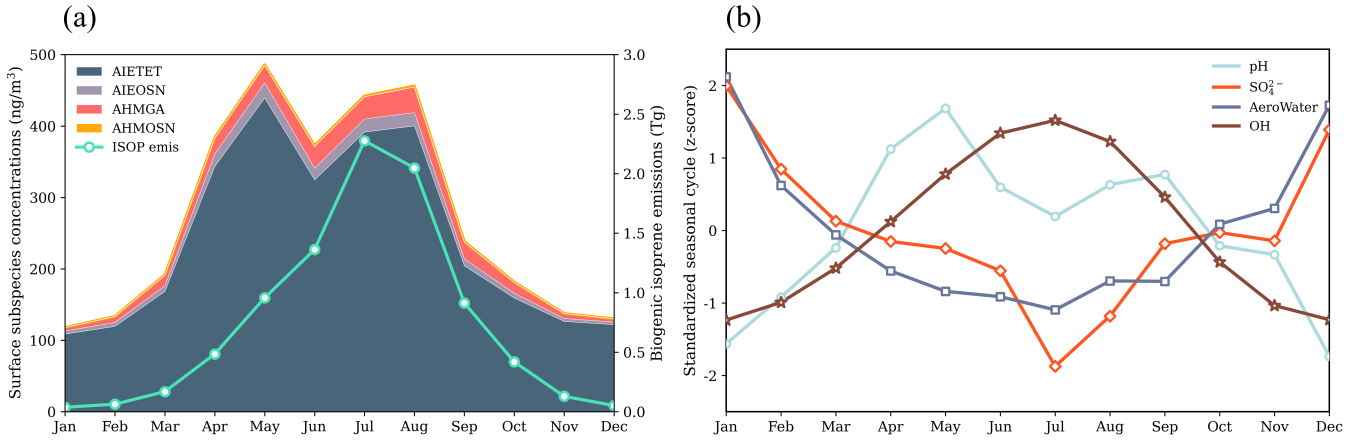

Figure 4: (a) Monthly variations of surface isoprene-derived secondary organic aerosol (ISOA) subspecies (left y axis; unit: ng m^{-3}) and biogenic isoprene emissions (ISOP emis; right y axis; unit: Tg) in China, based on the climatological monthly means averaged over the five simulation years (2000, 2006, 2012, 2016, and 2019). (b) Standardized monthly variations of background chemical and aerosol variables relevant to ISOA formation, including surface aerosol pH, surface sulfate (SO_4^{2-}) concentrations, surface aerosol liquid water (AeroWater) concentrations, and surface hydroxyl radical (OH) concentrations in China, based on the climatological monthly means averaged over the five simulation years.

Comment#12: [Table 1] It may be helpful to add a vertical line between the SWC and SGN results.

Response: We thank the reviewer for this helpful suggestion. We have revised the formatting of Table 1 by adding vertical lines between the Driver column, the SWC results, and the SGN results to improve readability and to more clearly separate the two regional result groups. We have also applied the same formatting style to Table S1 for consistency.

Comment#13: [Fig. 8] Include what the dashed curves represent in the figure caption.

Response: We thank the reviewer for pointing this out. In the previous version, the dashed curves in Fig. 8 represented least-squares linear trend lines fitted to the five selected simulation years for each species. In the revised manuscript, we have removed these dashed curves from Fig. 8 to avoid visual clutter and potential confusion. The purpose of Fig. 8 is now to show the temporal evolution and stage-to-stage variations of ISOA subspecies and related controlling factors in SWC and SGN across the selected simulation years. The long-term trend magnitudes are already presented in Fig. 7. Accordingly, the caption of Fig. 8 has been revised to describe only the solid time-series curves shown in the updated figure.

Comment#14: [Line 529] A closing parenthesis is missing.

Response: We thank the reviewer for pointing this out. We have added the missing closing parenthesis.

Comment#15: For clarity, I would replace the double-negative phrasing when describing percent changes ("decreased by -X%" → "decreased by X%" or "changed by -X%").

Response: We thank the reviewer for this helpful suggestion. We have checked the manuscript and revised the double-negative phrasing in the descriptions of percentage changes. Specifically, expressions such as “decreased by −X%” have been revised to clearer wording, such as “decreased by X%” or “changed by −X%,” depending on the context. These wording changes have been applied throughout the manuscript where applicable.